Oral Presentation at HTS-Workshop on Applications and New Materials
8-10 May 1995, Twente, The Netherlands

Hole-overdoped $Ca_xSm_{1-x}Ba_2Cu_3O_y$ bicrystal junctions and field effect transistors

Z. W. Dong, P. Hadley, V. C. Matijasevic, and J. E. Mooij

Applied Physics, Delft University of Technology, Delft, The Netherlands

Abstract

High-T_c Josephson field effect transistors (JoFETs) were fabricated using reactive molecular beam epitaxy. Thin films of $Ca_xSm_{1-x}Ba_2Cu_3O_y$ were deposited on bicrystal $SrTiO_3$ substrates and then gates were structured over the resulting junctions. The $Ca_xSm_{1-x}Ba_2Cu_3O_y$ superconducting electrodes were hole-overdoped while the grain boundary region was hole-underdoped. The I_cR_n product of the junctions was ~ 0.25 mV and critical current density was ~ 10^3 A/cm^2 at 4.2 K. The critical current of the junctions was modulated by the application of a gate voltage. The largest field effect was observed in films where 30% of the Sm was replaced by Ca. The critical current of the junction was modulated 26% by the application of an electric field of 5×10^5 V/cm.

Introduction

Great efforts have been devoted in the last few years to the development of high-T_c superconducting three terminal devices such as flux-flow transistors,[1] field effect transistors,[2,3] and quasiparticle injection devices.[4] Electric field effects in homogeneous ultrathin films have been widely studied. However, electric field effects in Josephson junctions have received less attention. In such a JoFET, an electric field is applied between the gate electrode and superconducting channel, which alters the charge carrier density n in the junction. The modulation in carrier density causes a modulation in the critical current. This device is expected to have a bigger field effect, and a faster switching speed than the other three terminal devices.[5]

One of the difficulties in fabricating the JoFETs is depositing a quality dielectric material on top of the high-T_c junctions. Some solutions to this problem that have been implemented are: using amorphous STO deposited at room temperature,[6] using an inverted structure with gate on the back of STO substrate,[7] or using a PMMA layer.[8] These experiments showed a field induced change in normal state resistance up to 5%, and a Josephson supercurrent enhancement of 20% - 70%. The maximum induced areal carrier density modulation is typically 10^{12} cm^{-2}. However, the sign of the field effect is not consistent in all of the experiments. Nakajima *et al.*[7] observed a decrease of the normal state resistance for negative gate voltages, $\Delta R_n/R_n = -\Delta N/N$. Ivanov *et al.*[6] observed enhancement of I_c at positive gate voltages rather than a reduction. The origin of field effects in a bicrystal junction is still unclear. The results reported here are consistent with the Nakajima result, indicating there is hole-underdoped material at the grain boundary.

Hole-overdoped $Ca_xSm_{1-x}Ba_2Cu_3O_y$ thin films and bicrystal junctions

Superconducting thin films of $Ca_xSm_{1-x}Ba_2Cu_3O_y$ (x = 0 - 40%) and heterostructures of Ca-SBCO/STO/Au and Ca-SBCO/BTO/Cu for high-T_c three terminal devices were deposited using a reactive molecular beam epitaxy system.[9] The optimal conditions for the growth of *c*-axis thin films were as follows: substrate temperature at 750 °C, total deposition rate of 0.1 - 0.2 nm/s and an ozone flux of 1.1×10^{15} /(cm^2-sec). The T_c of films ranged from 50 - 92 K for different Ca-dopings. When Ca^{2+} was substituted for Sm^{3+} in 123-SBCO system, it induced additional holes in the CuO_2 planes and made the Ca-SBCO hole-overdoped. The overdoped films have been studied by a series of successive anneals at 450 °C at subatmospheric oxygen pressure, in which the T_c of the 40% doped film increased by 20 K before it went down again upon successively reducing the oxygen content.[3,9] Furthermore, we have measured the sign of the field effect in such an ultrathin film and it was consistent with the films being hole-overdoped since an increase in T_c was observed when applying a positive voltage to the gate. The degree of overdoping was controlled by changing the Ca content. This allows one to optimize the carrier density to maximize the field effect. For a maximum field effect, the material should be away from the optimal doping where T_c is maximum but dT_c/dn is zero, and be as close to a maximum of the slope, dT_c/dn, as possible. In addition, the overdoped films provide a way to separate the field effects on grain boundaries from those on the films since weak links formed at grain boundaries are known to be underdoped due to oxygen depletion.[10] All of the films which were used in this paper to investigate field effects were 50 nm thick. This ensures that the films were of high quality and did not contain additional grain boundaries.

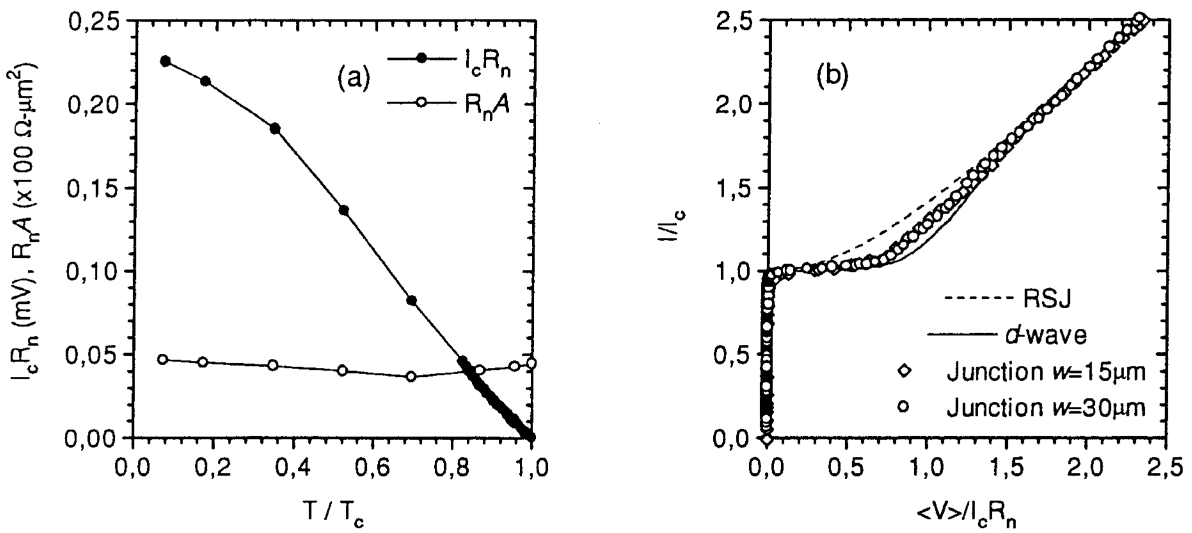

Figure 1: (a) Typical I_cR_n and R_nA values as a function of temperature for hole-overdoped $Ca_{0.3}Sm_{0.7}Ba_2Cu_3O_y$ bicrystal junctions ($w = 30\,\mu$m). The tilt angle of the bicrystal is 24°. (b) *I-V* characteristics of *d*-wave tunnel junctions (solid line) at $T = 0$ K,[11] *s*-wave junctions with RSJ model (dashed line) and $Ca_xSm_{1-x}Ba_2Cu_3O_y$ bicrystal junctions (data points) at 10 K.

Bicrystal Josephson junctions were made by depositing Ca-doped SBCO superconducting thin films on 24° tilted bicrystal (100) $SrTiO_3$ substrates. The junctions had a lower critical current density and a higher resistance than as-made hole-underdoped YBCO bicrystal junctions with the same grain boundary tilt angle. Upon increasing the doping in the electrodes, the T_c of junctions decreased while the junction resistances only slightly increased. The normal resistance of bicrystal junctions was rather high, ~ 5 Ω-μm^2, and temperature independent over a wide range of temperature. The I_cR_n was linearly dependent on T and had value of ~ 0.25 mV at 4.2 K. Figure 1(a) shows the temperature dependencies of the junction resistances and I_cR_n values. Typically, junctions at high temperatures exhibit RSJ-like behavior in both *dc*- and *ac*-

characteristics. However, junctions at low temperatures showed a sharper rise in voltage than predicted by the RSJ model, as can be seen in Fig. 1(b). The reason for this seems to be related to *d*-wave superconductivity. Recently, van Otterlo *et al.*[11] have generalized the Ambegaokar-Baratoff calculation to include tunneling between superconductors with various pairing states. The calculated *I-V* curve for zero misorientation of the crystal axes at 0 K is reprinted in Fig. 1(b) as a solid line. This *I-V* curve is very similar to those measured on our bicrystal junctions.

Josephson field effect transistors

Using hole-overdoped Ca-SBCO bicrystal junctions, we have made high-T_c three terminal devices, Josephson field effect transistors.[8,9] A schematic cross-section of the samples is shown in Fig. 2 along with a measurement circuit. The superconducting drain and source electrodes are connected by the grain boundary junction. The devices were defined using photolithography and Ar ion milling. To insulate the gate electrode, either a 200 nm thick amorphous $SrTiO_3$ film (a-STO) was deposited at room temperature by MBE through a resist lift-off mask, or a 1 μm thick polymethylmethacrylate (PMMA) layer was spun on over the grain boundary junction. PMMA has nearly the same dielectric constant as SiO_2, but the breakdown field of PMMA is much higher than that of SiO_2. Therefore it is often employed as an insulating layer in the metallization of GaAs devices.[12] A 100 nm thick Au or Cu gate was then deposited on top of these insulators. The widths of devices used were 3, 5, 10, 15, 20, 30, and 50 μm and the J_c of junctions was about 10^3 A/cm^2 in zero applied electric field at 4.2 K.

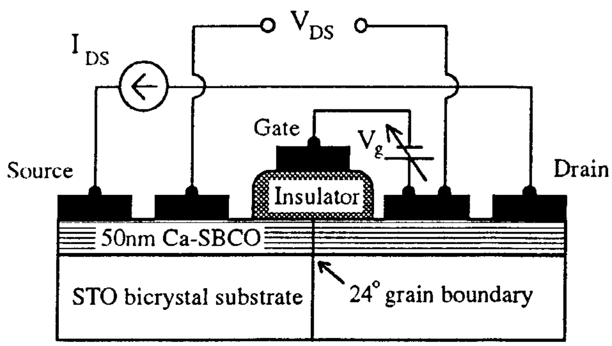

Figure 2: A schematic of Josephson field effect transistors and a circuit outline for the field effect measurements.

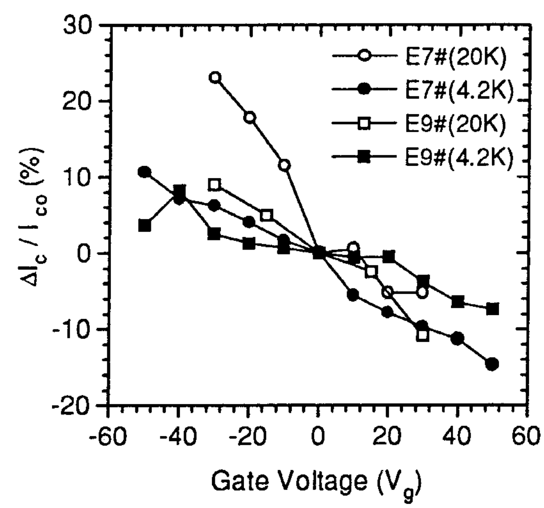

Figure 3: Electric field modulation of normalized critical current as a function of the applied gate voltage for the devices with 30% Ca-doped SBCO electrodes at 20 K (open data) and at 4.2 K (solid data). The circles represent the 15 μm wide device and the squares represent the 30 μm device.

The gate voltage, V_g, was applied by using a battery in order to keep the noise as low as possible. The gate voltage was varied from −50 V to +50 V. When a negative voltage was applied to the gate, extra holes were added to the junctions. In contrast, a positive gate voltage induced hole filling and the carrier density decreased. The breakdown field for a-STO was asymmetric. The breakdown occurs at +14 V and –2 V for a 200 nm thick a-STO at 40 K, corresponding to breakdown fields (E_{BD}) of $+7\times10^5$ V/cm and -1×10^5 V/cm, respectively. For the devices with PMMA as the dielectric layer, the breakdown voltage was above ±50 V which was the limit of the voltage source. This means that the E_{BD} for the PMMA layer is greater than 5×10^5 V/cm at low temperatures. All of the experiments were carried out with gate leakage current below 1 nA.

The current-voltage characteristics of many devices for undoped and Ca-doped samples were measured at different gate voltages and different temperatures. In all of these measurements, a positive gate voltage decreased both the I_c and the T_{co} while a negative gate voltage increased I_c and T_{co}.[8,9] This is consistent with an underdoped weak link at the grain boundary which dominates the transport. The largest field effect was observed for the devices with 30% Ca-doped SBCO electrode and PMMA gate dielectric, where the T_{co} shift was about 8 K. Figure 3 shows the dependence of the normalized critical current on the applied gate voltage. At 4.2 K, an I_c modulation of 26% for a gate voltage modulation from –50 V to +50 V was obtained. The modulation of the critical current at 20 K was larger than that at 4.2 K. At 20 K, the critical current increased 23% for a gate voltage of –30V and decreased 6% for a gate voltage of +30V. Since the hole-overdoped electrodes would cause a shift in I_c with the opposite sign, we attribute the entire modulation observed here to the electric field in the hole-underdoped grain boundary junction.

Charge modulation in a bicrystal junction

The $\varepsilon_r E_{BD}$ products are on the order of 10^6 V/cm for both PMMA and a-STO dielectric layers. Such low $\varepsilon_r E_{BD}$ products only induce very small changes in the areal carrier density, $\Delta N_{max} = \varepsilon_o \varepsilon_r E_{BD} \approx 1.5\times10^{12}$ cm^{-2}. The capacitances per unit area are 5 nF/cm^2 for PMMA and 50 nF/cm^2 for a-STO. This results in an induced charge density, $\Delta N/V_g$, of about 3.2×10^{10} cm^{-2}V^{-1} for PMMA and 3.2×10^{11} cm^{-2}V^{-1} for a-STO. The electric field necessary to modulate the critical current density in these bicrystal junctions is about one hundred times less than the electric field necessary in a homogeneous thin film. One reason for this is that the carrier density in the grain boundary region is lower than in a homogeneous film. Due to oxygen loss, the grain boundary may have a carrier density that is less than 10^{20} cm^{-3}.[7,10]

In order to fully understand the large field effect, it is necessary to understand the nonsuperconducting region at the grain boundary. The observed field effect indicates that the nonsuperconducting region is wider than the electric penetration depth. If this was not so, the superconducting electrodes would screen the applied field and keep it from penetrating into the grain boundary region. This picture is reinforced by TEM-EELS measurements which show that there is a region of oxygen deficiency around the grain boundary.[10] The width of this region is related to the angle of the grain boundary. For a 24° grain boundary junction, this width was found to be about 20 nm. Since the oxygen content is closely related to the carrier concentration in this material, the carrier concentration must be modulated over the same distance as the observed oxygen depletion region.

The observed critical current density also provides some information about the nature of the grain boundary. For weak coupling between the superconducting electrodes, the critical current density is proportional to $\exp(-d/\xi_n)$, where d is the spacing between the superconducting electrodes and ξ_n is the normal metal coherence length. The critical current in the bicrystal junction was measured to be 10^3 A/cm^2 which is about six orders of magnitude

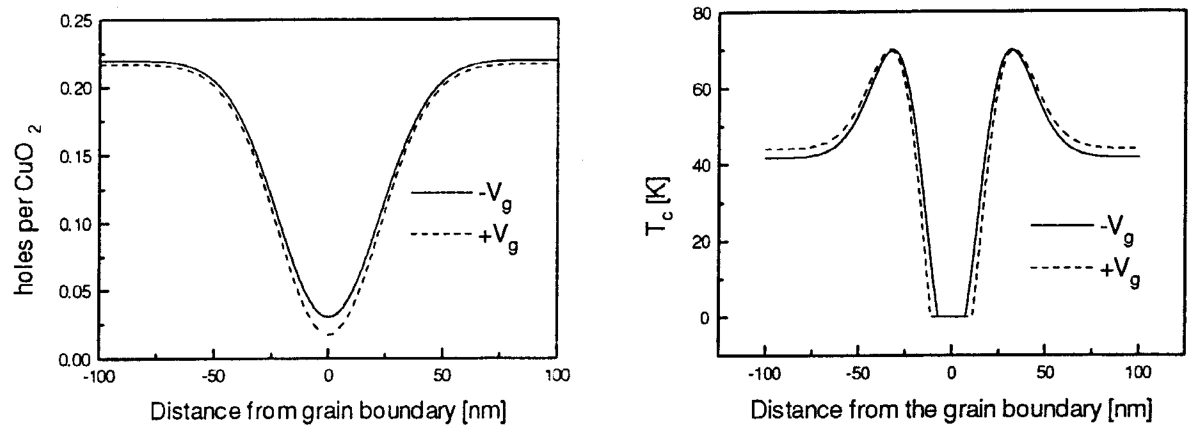

(a) (b)

Figure 4: (a) The carrier density of a Ca-SBCO film near a grain boundary junction for several values of the gate voltage. (b) The local $T_c(x)$ near the grain boundary.

lower than the depairing critical current density. This indicates that the ratio d/ξ_n must be about 13. For a nonsuperconducting region of 20 nm wide, $\xi_n \approx 2$ nm.

Figure 4(a) shows schematically how the carrier density near the grain boundary could be modulated as a function of the applied gate voltage. The modulation is the greatest near the grain boundary where the carrier density is the lowest. The carrier density determines the superconducting properties of the film. The relation between the carrier density, n, and T_c for the cuprates is parabolic and is believed to be the following, $T_c = T_{c,max}(1 - 82.6(n - 0.16)^2)$,[13] where $T_{c,max} \approx 70$ K for 30% Ca-doped SBCO films.[3] From the carrier density, one can define a local critical temperature, $T_c(x)$, which is the T_c of a homogeneous film with the same carrier density as the JoFET at position x. This local $T_c(x)$ is plotted in Fig. 4(b). The temperature where the device displays a supercurrent can be higher than the minimum of $T_c(x)$ due to the proximity effect. Far from the grain boundary, the SmBaCuO film is overdoped so $T_c(x)$ does not obtain its maximum value. Near the grain boundary, the film is underdoped and $T_c(x)$ goes to zero. The local critical temperature goes through a maximum on the two sides of the grain boundary where the carrier density obtains its optimum value. The application of an electric field modulates the width of the region where $T_c(x)$ is suppressed. Since the critical current depends exponentially on this width, the electrical field has a strong effect on the critical current density. However, it is not just the spacing between the two superconducting electrodes that is modulated by the electric field. The normal metal coherence length is also a function of the carrier density. The coherence length decreases as the carrier density decreases. The modulation of the critical current density depends on both the modulation of the spacing between the superconducting electrodes and the modulation of the normal metal coherence length.

Conclusions

Josephson field effect transistors have been made by depositing hole-overdoped $Ca_xSm_{1-x}Ba_2Cu_3O_y$ thin films on bicrystal substrates and structuring gates on the resulting junctions. By inducing a surface carrier density of 10^{12} holes/cm^2 we measured a modulation in

I_c of 29% at 20 K and 26% at 4.2 K. The sign of the field effect indicates that the critical current of the device was dominated by a hole-underdoped region near the grain boundary. The electric field which is necessary to modulate the critical current was much smaller than is necessary for a similar modulation of thin films without grain boundaries. This is explained in terms of a modulation of the Josephson coupling between the electrodes.

References

1. J.S. Satchell, *et al.*, Elec. Lett. **28**, 781 (1992); J. Schneider, *et al.*, Appl. Phys. Lett. **63**, 2426 (1993) or EUCAS'93 page 1151; L. Alff, *et al.*, J. Appl. Phys. **75**, 1843 (1994).
2. J. Mannhart, D.G. Schlom, J.G. Bednorz and K.A. Muller, Phys. Rev. Lett. **67**, 2099 (1991); X.X. Xi, Q. Li, C. Doughty, C. Kwon, S. Bhattacharya, A.T. Findikoglu and T. Venkatesan, Appl. Phys. Lett. **59**, 3470 (1991) or Phys. Rev. Lett. **69**, 2709 (1992); K. Joosse, Yu.M. Bouguslavskij, G.J. Gerritsma, H. Rogalla, J.G. Wen and A.G. Sivakov, Physica C **224**, 179 (1994).
3. V. Matijasevic, S. Bogers, N.Y. Chen, H.M. Appelboom, P. Hadley and J.E. Mooij, Physica C, **235-240**, 2097 (1994) and Proceedings of EUCAS'93, p 655.
4. T. Kobayashi, K. Hashimoto, U. Kabasawa and M. Tonouchi, IEEE Trans. Magn. **25**, 927 (1989); Yu.M. Bouguslavskij, K. Joosse, A.G. Sivakov, F. Roesthuis, G. Gerritsma and H. Rogalla, Physica C **220**, 195 (1994).
5. A.W. Kleinsasser, "*The New Superconducting Electronics*", H. Weinstock and R.W. Ralston (Eds), NATO ASI Series E, Vol. 251, 249 (1993); J. Mannhart, Proceedings of Workshop on HTS Josephson Junctions and 3-Terminal Devices, p. 22, University of Twente, Enschede, The Netherlands, May 2-4, 1994.
6. Z.G. Ivanov, E.A. Stepantsov, A.Y. Tzalenchuk, R.I. Shekhter and T. Claeson, IEEE Trans. Appl. Supercond. **3**, 2925 (1993).
7. K. Nakajima, K. Yokota, H. Myoren, J. Chen and T. Yamashita, Appl. Phys. Lett. **63**, 684(1993) and Jpn. J. Appl. Phys. **33**, L934 (1994).
8. Z.W. Dong, V.C. Matijasevic, P. Hadley, S.M. Shao and J.E. Mooij, presented at ASC'94 in Boston, USA, October 16-21, 1994, will be published in IEEE Trans. Appl. Supercond.
9. Z.W. Dong, "*High-T_c Superconducting Thin Film Devices*", Ph.D. dissertation, Applied Physics, Delft University of Technology, April 18, 1995.
10. N.D. Browning, J. Yuan and L.M. Brown, Physica C, **202**, 12 (1992) and Physica C, **212**, 185(1993); J. Betouras and Robert Joynt, to be published, March, 1995; Z.L. Wang, *et al.*, Phys. Rev. B **48**, 9726(1993), and Interface Science, 1 (1994).
11. C. Bruder, A. van Otterlo and G.T. Zimanyi, to be published.
12. C.R.M. Grovenor, "*Microelectronic Materials*", p 312.
13. J. Tallon and N. Flower, Physica C, **204**, 237 (1993).